

Finite Difference Method for Mechanical Adaptation of Arteries to Sustained Hypertension

Dr. Mahesh Chandra¹ and Mr. Krishna Gopal²

¹Assistant Professor, Department of Mathematics, FS University, Shikohabad, (U.P.), INDIA.

²Department of Mathematics, FS University, Shikohabad, (U.P.) INDIA

¹Corresponding Author: maheshchandra2047@gmail.com



www.jrasb.com || Vol. 4 No. 2 (2025): April Issue

Received: 23-03-2024

Revised: 28-03-2024

Accepted: 03-04-2024

ABSTRACT

The dynamics of arterial wall remodelling under hypertensive conditions is discussed here. Sustained hypertension was simulated by a step increase in blood pressure. The arterial wall was considered to be a thick walled tube made of non linear elastic incompressible material the driving stimuli for the geometric adaptation are the normalized deviations of wall stresses from their values under normotensive conditions. Mechanical adaptation is driven by the difference between the area compliance under hypertensive and normotensive conditions. The predicted time course of the geometry and mechanical properties of arterial wall are in good qualitative agreement with published findings. Crank Nicolson finite difference scheme is used for computation purpose which is fast converging in comparison to the method used by Rachev et al (1998).

Keywords- Hypertension, Adaptation, Incompressible.

I. INTRODUCTION

There exists an increasing interest in the investigation of changes that appear in the geometry structure and mechanical properties of the arterial wall when the vessels are subjected to abnormal pressure and flow conditions (Rachev et al 1998). Understanding of the processes of arterial adaptation is of importance because it has been postulated that some pathological states might be considered as a result of remodelling gone into wrong direction (fung et al. 1993)

Experimental studies on geometric and oral recognition of terrainal pears Ave been carried out in several directions bors have tidied De adaptive response of the vascular wall to change in bed flow increase of the wall thickness and a reduction of the il riu lengphudimal thretch ratio of dogs aasta due to sustained hypension has been observed by vaishnave (1990)

Coupling between grametric and mechanical moshuarities in the process of arterial wall deformation enhances the complexity in the adaptation proosdire described above. Thickening of the arterial wall in

response to increased pressure causes a change of the defensed arterial radius. Then, even when the flow is kept constant, the shear stress at the arterial endothelium is altered which engages mechanisme for the adaptation of the inner radius. On the other hand any change of mechanical properties of the vascular material causes changes in the stress and strain distribution in the arterial wall even when the artery is subjected to constant fond.

An efficient approach to better understanding and assessment of the contribution of different factors involved in arterial wall as well as interrelation between them, in the mathematical modelling and numerical simulation of the process of remodelling under altered pressure or flow conditions

A different approach to study the dynamics of the geometric remodelling in response to changes in blood pressure has been applied by Rachev et al (1996).

They studied the dynamics of geometric adaptation in response to change in blood pressure. It was assumed that during remodelling the zero-stress configuration of the arterial cross section remains a circular sector. The wall changes only its geometric

dimension while the material properties remain the same.

Governing Equations:

For incompressible wall material and radial, circumferential and axial stretch ratio are given by

$$R_i = \frac{H}{m-1}, R_o = \frac{mH}{m-1}, \phi = \pi - \frac{L_o - L_t}{2H} \quad \text{where } m = \frac{L_o}{L_t} \quad \dots\dots\dots(1)$$

$$\lambda_r = \frac{R}{\lambda_t}, \lambda_\theta = \frac{r}{R}, \lambda_z = \lambda \quad \dots\dots\dots(2)$$

where $\chi = \pi/\pi - \phi$, r and R are the radial co-ordinates of an arbitrary point in the deformed and zero stress state respectively, being related through the equation

$$\gamma = \sqrt{\frac{R^2 + r^2}{\lambda_t^2 + \lambda_z^2} (\mu^2 - \lambda_z^2)} \quad \dots\dots\dots(3)$$

The deformation parameters μ and λ are defined as

$$\mu = \frac{r}{R_i}, \lambda = \frac{L_t}{L} \quad \dots\dots\dots(4)$$

with r_i being inner radius in the deformed state and L_t and L being the length of the arterial segment at deformed and zero-stress state respectively. The non vanishing components of the green strain tensor are $e_j = \frac{1}{2}(\lambda_j^2 - 1)$ ($j = r, \theta, z$)

The radial, circumferential and longitudinal stresses are given by

$$\sigma_r = \lambda_r^2 \frac{\partial W}{\partial e_r} + q, \quad \sigma_\theta = \lambda_\theta^2 \frac{\partial W}{\partial e_\theta} + q, \quad \sigma_z = \lambda_z^2 \frac{\partial W}{\partial e_z} + q \quad \dots\dots\dots(6)$$

where $W(e_r, e_\theta, e_z)$ is the strain energy function which completely describe the mechanical properties of the wall material q is the unknown scalar function that has to be determined from the equilibrium equation and boundary conditions.

After integration of the differential equations of equilibrium and imposing the boundary conditions for the internal surface $\sigma_r(r = r_1) = -p$ and the outer surface $\sigma_r(r = r_o) = 0$ the following expression for the wall stresses are obtained

$$\sigma_r = \int_{r_1}^r \left(\lambda_\theta^2 \frac{\partial W}{\partial e_\theta} - \lambda_r^2 \frac{\partial W}{\partial e_r} \right) \frac{dr}{r} - p$$

$$\sigma_\theta = \sigma_r + \lambda_\theta^2 \frac{\partial W}{\partial e_\theta} - \lambda_r^2 \frac{\partial W}{\partial e_r} \quad \dots\dots\dots(7)$$

$$\sigma_z = \sigma_r + \lambda_z^2 \frac{\partial W}{\partial e_z} - \lambda_r^2 \frac{\partial W}{\partial e_r}$$

where r_i and r_o are the deformed inner and outer radius, respectively. Pressure p and the axial force F_z relate to wall stresses given below.

$$p = \int_{r_1}^{r_o} \left(\lambda_\theta^2 \frac{\partial W}{\partial e_\theta} - \lambda_r^2 \frac{\partial W}{\partial e_r} \right) \frac{dr}{r}, \quad F_z = 2\pi \int_{r_1}^{r_o} r \sigma_z dr \quad \dots\dots\dots(8)$$

The Average Circumferential axial stresses are given below

$$\sigma_{\theta av} = \frac{p_i}{r_o - r_i}, \quad \sigma_{z av} = \frac{F_z}{\pi(r_o^2 - r_i^2)} \quad \dots\dots\dots(9)$$

The mean shear stress at the inner arterial surface is given by Poiseuille's law.

$$\tau = \frac{4\eta Q}{\pi r_1^3} \quad \dots\dots\dots(10)$$

where Q is flow and η blood viscosity.

II. REMODELLING RATE EQUATIONS

Following Rachev et al (1998) the artery is first considered under normotensive conditions. The

dimensions at the zero stress state are L_N, L and L_H . Superscripts N and H denote the values under normotensive and hypertensive conditions respectively, the vessel is subjected to normal blood pressure p^N and is kept at constant deformed length. Induced arterial hypertension is modeled by a step increase in blood pressure from p^N to p^H . Blood flow rate is kept constant. To monitor the remodelling of zero-stress state, the following growth parameters are defined.

$$\alpha(t) = \frac{L_t^H(t)}{L_t^N}, \quad \beta(t) = \frac{L_o^H(t)}{L_o^N}$$

$$\gamma(t) = \frac{H^H(t)}{H^N}, \quad \delta(t) = \frac{L_t^H(t)}{L_t^N} \quad \dots\dots\dots(11)$$

It is postulated that the artery remodels its zero-stress configuration in a manner to restore the distribution of circumferential stress and the magnitude of the average axial stress as they are under normotensive condition. Since circumferential stresses vary smoothly through out the arterial wall the following remodeling rate equation for the growth parameters are postulated.

$$\frac{d\alpha}{dt} = \frac{1}{t_c} \left[\frac{\sigma_r^H(t) - \sigma_r^N}{\sigma_r^H} \right] \quad \dots\dots\dots(12)$$

$$\frac{d\beta}{dt} = \frac{1}{t_c} \left[\frac{\sigma_\theta^H(t) - \sigma_\theta^N}{\sigma_\theta^H} \right] \quad \dots\dots\dots(13)$$

$$\frac{d\gamma}{dt} = \frac{1}{t_H} \left(\frac{\sigma_{\theta av}^H(t) - \sigma_{\theta av}^N}{\sigma_{\theta av}^H} \right) \quad \dots\dots\dots(14)$$

$$\frac{d\delta}{dt} = \frac{1}{t_c} \left(\frac{\sigma_{z av}^H(t) - \sigma_{z av}^N}{\sigma_{z av}^H} \right) \quad \dots\dots\dots(15)$$

$$\frac{\partial \sigma_{\theta av}^H}{\partial c} \frac{dc}{dt} + \frac{\partial \sigma_{\theta av}^H}{\partial b_1} \cdot \frac{db_1}{dt} + \frac{\partial \sigma_{\theta av}^H}{\partial b_2} \cdot \frac{db_2}{dt} = 0 \quad \dots\dots\dots 16$$

$$\frac{\partial \sigma_{z av}^H}{\partial c} \frac{dc}{dt} + \frac{\partial \sigma_{z av}^H}{\partial b_1} \cdot \frac{db_1}{dt} + \frac{\partial \sigma_{z av}^H}{\partial b_2} \cdot \frac{db_2}{dt} = 0 \quad \dots\dots\dots 17$$

where $\sigma_r^H(t), \sigma_\theta^H(t), \sigma_{\theta av}^H(t)$ and $\sigma_{z av}^H(t)$ are the current circumferential stress at the inner surface. The stress at the outer surface, the average circumferential and the average axial stress of the hypertensive artery $\sigma_r^N, \sigma_\theta^N, \sigma_{\theta av}^N$ and $\sigma_{z av}^N$ are corresponding stress in the normotensive artery. t_c, t_H and t_z are characteristic time constants. C_A^N and $C_A^H(t)$ are the area compliance. $C_A = \frac{\Delta A}{A \Delta p}$ (Cow and Taylor 1960)

The mismatch between these compliance plays the role of a driving stimulus for the change of the material constant c . Following the introduced hypothesis for the compatibility between geometric and mechanical adaptation. It is accepted that the constant b_1 and b_2 vary in a manner to maintain the current level of the average circumferential and average axial stress. This implies that at any moment the rate of change of the average stresses with respect to the variables material constant c, b_1 and b_2 respectively which yields

Applying Crank-Nicolson scheme in the above equations, the above equations become in the discretized form as follows:

The aim of this study is to propose a relatively simple but general mathematical model, using Crank-Nicolson Scheme which accounts for both the geometric and mechanical remodelling of arteries in response to induced hypertension. Theoretical predictions of the model are compared against available experimental data to assess the validity of certain new hypothesis concerning the driving stimuli and interrelation between wall-stress-dependent compliance adaptation.

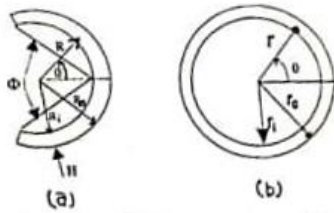


Figure 1. Schematic diagram of an artery at (a) zero-stress state and (b) loaded state

The artery is considered to be a thick walled tube made of non-linear, elastic orthotropic and incompressible material. At the zero stress state the vessel cross-section is considered to be a circular sector with the following dimensions. Inner arc length L_1 , outer arc length L_0 and thickness H . The inner and outer radii of curvature (R, R) and the opening angle ϕ . are calculated using the formulae.

Schematic diagram of an artery at (a) zero stress state (b) loaded state under physiological loading, arteries are in a finite axisymmetric plane strain state. The deformed arterial cross section is shown in fig (b)

$$\frac{1}{4\Delta c} \left(\sigma_{\theta}^{k+1} - \sigma_{\theta}^k \right) \frac{1}{\Delta t} \left(c_{i+1}^{k+1} - c_{i-1}^{k+1} + c_{i+1}^k - c_{i-1}^k \right) + \frac{1}{4\Delta b_1 \Delta t} \left(b_{1i+1}^{k+1} - b_{1i-1}^{k+1} + b_{1i+1}^k - b_{1i-1}^k \right) \left[\sigma_{\phi_{iav}}^{k+1} - \sigma_{\phi_i}^k + \sigma_{\phi_{iav}}^{Hk+1} - \sigma_{\phi_{iav}}^H \right] \dots\dots\dots 18$$

$$\frac{1}{4\Delta c} \left(\sigma_z^{k+1} - \sigma_z^k \right) \frac{1}{\Delta t} \left(c_{i+1}^{k+1} - c_{i-1}^{k+1} + c_{i+1}^k - c_{i-1}^k \right) + \frac{1}{4\Delta b_1 \Delta t} \left(b_{1i+1}^{k+1} - b_{1i-1}^{k+1} + b_{1i+1}^k - b_{1i-1}^k \right) \left[\sigma_{z_{iav}}^{k+1} - \sigma_z^k + \sigma_{z_{iav}}^{Hk+1} - \sigma_{z_{iav}}^H \right] \dots\dots\dots 19$$

III. NUMERICAL METHOD

The system of equations (13) to (19) are highly non linear because all variables depend on complex manner on the geometric parameter of the current zero-stress configuration and elastic properties. More over equations (13) to (17) are coupled and have to be solved simultaneously with the equations (2) to (10) for inflation at pressure P^H and longitudinal extension λ , at $t = 0$ when the pressure is increased in step wise manner from P^N to P^H

The initial value for the growth parameters is $\alpha = \beta = \gamma = \delta = \xi = 1$. The values of the inner deformed radius stresses and the compliance $C_{\{A\}}$ Change in a stepwise manner when the pressure increase from P^N to P^H and are calculated using the dimensions of the normotensive artery subjected to the hypertensive pressure at the normotensive in situ, longitudinal axial stretch ratio λ .

The problem of determining the functions $\alpha(t)$, $\beta(t)$, $\gamma(t)$ and $\delta(t)$ from the governing equations and initial conditions $\kappa(0) = \beta(0) = \gamma(0) = \delta(0) = \xi$ a single valued solution making use of equation (1) it is possible to determine

that time variations of the dimensions of the zero stress configuration of the arterial cross section and the longitudinal stretch ratio. Solving equations (18) and (19) it is possible to obtain the time course of the elastic properties of the artery also. The integration of (16) to (19) accounts for the flow-induced adaptation of the artery. Equation (16) & (17) are solved by Crank-Nicolson Scheme.

IV. RESULTS AND DISCUSSION

A numerical study using data available in the literature was performed. Data for zero-stress configuration strain energy function for a rabbit thoracic aorta were taken from the paper chung and Fung (1986). The dimensions of the zero stress state are $L_0 = 11.25$ mm $L_i = 9.75$ mm -1086 degree they were accepted to correspond to the homeostatic case in which the artery is subjected to an arterial pressure of $P^{\prime} = 13.33k * P_{\{4\}}$ and in situ axial stretch of the material constants $c = 22.4$ kpa $b_{\{1\}} = 1.0672$, $b_{\{2\}} = 0.4775$, $b_{\{3\}} = 0.0499$, $b_{\{4\}} = 0.903$, $b_{\{z\}} = 585$ dot $y - x = 1.6$, $b_{\{s\}} = 0.0042$ for purpose qualitative analysis. (See Rachev et al (1998)), induced hypertension is simulated by a step increase to a pressure of $p^H = 21.33$ kpa.

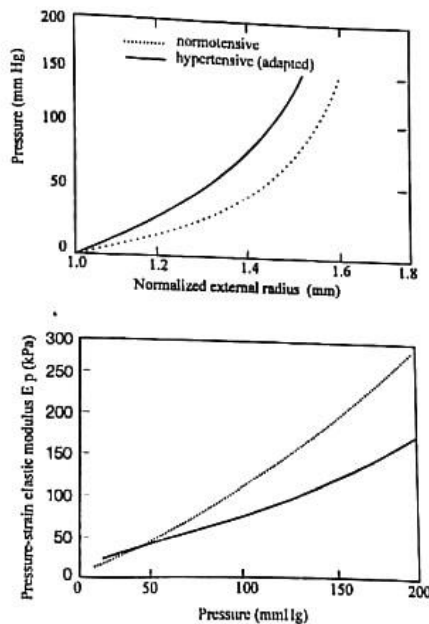
The present study predicts a monotonic steady state approximately 50% higher than the thickness of the normotensive aorta. The time course of the opening angle shows very rapid increase, reaching a maximum, after which the angle decrease to an asymptotic value.

The present study utilizes a phenomenological model for wall remodelling in which stress-driven processes at the molecular cellular and tissue levels are all lumped in to remodelling rate equations linking the cause (stresses) and the effect (remodelling) this is of course, an over simplifications of the underlying biology in order to yield mathematically simple models. In reality, however the adaptation to stress and wall shear are fundamentally different, wall stress induces growth principally through smooth muscle hypertrophy, while increased initial shear leads to proliferation of smooth muscle cells.

The pressure-outer radius relationships of Fig. 2(a) show the theoretical prediction of the response of the normotensive and adapted hypertensive aorta inflated at in situ length. The curves represent the mechanical behaviour of the vessels incorporating both the inherent elastic properties of the vascular material and the geometric dimensions at the zero-stress state. The results are in good agreement with experimental findings of Matsumoto and Hayashi (1994) and Rachev et al (1998).

The use of Crank Nicolson Scheme saves a lot of computer time. These simulation have been performed in Pantium II. Linearized mechanical response of the arteries expressed in terms of the

Peterson pressure-strain elastic modulus is shown in fig. 2(b).



Figures 2: (a) and 2(b) illustrate the time variations of the compliance, $C_{\{A\}}$, and Peterson modulus, $E_{\{p\}}$ respectively

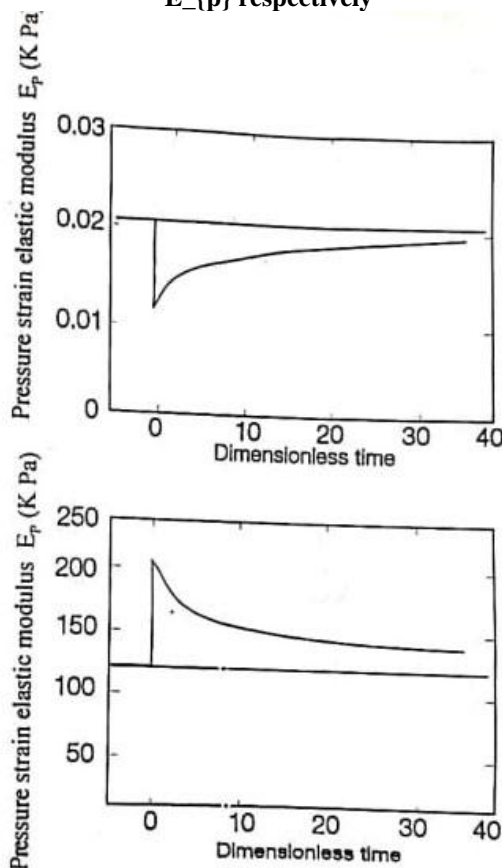


Fig. 3 (a) Pressure-normalized outer radius curves of the normotensive and hypertensive (adapted) aorta; (b) Pressure-strain elastic modulus versus pressure for normotensive and hypertensive (adapted) aorta

In brief the proposed scheme is found simple and most satisfying.

REFERENCES

- [1] Agonafer, D., Watkins, C.B. Cannon, J.N. (1985) - Computation of steady flow in a two dimensional arterial model. J. Biomechanics Vol. B. No. 9. pp. 695-701.
- [2] Bhardwaj, B.K. Mabon, R. F. and Giddens. D.O. (1982)-Steady flow in a model of the human carotid bifurcation. Part 1 Flow visualisation J Biomechanics, 15, pp. 349-362.
- [3] Bitoum, J.P. and Bellet, D. (1986) Blood flow through a stenosis in microcirculation- Biorheology-23, pp. 51-61.
- [4] Chakrabarty, S. And Dutta, A. (1992) Pulsatile blood flow in a porous stenotic artery using a suitable mathematical model. Mathematical Computation Modelling, Vol. 16, No. 2, pp. 35-54.
- [5] Chakrabarty, S. and Dutta, A-: (1992b)Dynamic response of stenotic blood flow in vivo. Mathematical Computational Modelling. Vol. 16, No. 2, pp. 3-20.
- [6] Chang, L.J. and Tarbell, J.M. (1985) Numerical simulation of fully developed sinusoidal and pulsatile (physiological) flow in curved tubes. J. Fluid Mechanics, 161, pp. 175-198.
- [7] Chaturani, P-and Swamy, R. (1986) - Pulsatile flow of Casson's flow through stenosed arteries with application of blood flow Biortheology, 23, pp. 499-511.
- [8] Chein, S., Usmani, S. and Skalak, R. (1984) Blood flow in small tubes. In handbook of Physiology. The cardiovascular system IV, ED. EM. (Renkin, C.C., Michel,). pp. 217-49.
- [9] Chein, S., Feng, SS., Vayo, M., Sung, LA, Usmanis, Skalak, R. (1988) The dynamics of shear disaggregation of RBC in the flow channel. Brotheology
- [10] Cokelet, G.R. (1986) Blood flow through arterial microvascular bifurcation in microvascular network. Experimental and theoretical studies, ec A.S. Popel, P.C. Jhonson, pp. 155-67, New York, Karger
- [11] Davids, N. and Ray, G. (1971) Finite element analysis of blood flow dynamics. The penn State University, Engineering Research Bulletin. B 102, pp. 1-54.
- [12] Ehrlich, L.W. (1979) The numerical solution of a Navier-Stokes problem in a stenosed tube. Computational Fluids, 7, pp. 247-256.
- [13] Fry, D.L. (1969)-Certain historical and chemical responses of the vascular interface to acutely induced mechanical stress in the aorta of dog Circulation Res. 24, pp. 93-108.

- [14] Garner, J.B. and Kellogg, R.B. (1989) Existence and uniqueness at the solution in general multisolute renal flow problem. *J. Math Bio*, 26, No. 4, pp. 455-464.
- [15] Gokhle, V.V., Tanner, R.I. and Bischoff, K. B. (1978) Finite element solution of the Navier Stokes equations for two dimensional steady flow through a section of a canine aorta model. *J. Biomechanics* Vol. 11, pp. 241-249
- [16] Haldar, K. & Ghosh, S.N. (1994), "Effect of a magnetic field on blood flow through an indented tube in the presence of erythrocytes, *Indian J. Pure and Applied Maths* 25 (3) pp. 345-352.
- [17] Hechmath, R.I. (1987) Properties of red blood cells in hand book of bioengineering, ed. R. Skalak, S. Chien, Vol. 17, pp. 1-12, New York, McGraw-Hill.
- [18] Jacques, M., Hugghe. C. Oomens, W. (1989), A low Reynolds number steady state flow through a branching network of rigid vessels LA Measure theory. *Biorheology* 26, pp. 55-71.
- [19] Kawai, H., Sawada, T. and Tanahashi, T. (1987). Numerical analyses of flow in a stenosed tube, proceeding of the second International conference on physiological fluid dynamics.
- [20] Karino, T. Motomiya, M. and Goldsmith, H.L.. (1990) - Flow patterns at the major junctions of the dog descending aorta. *J. Biomechanics* 23, pp. 537-548.
- [21] Krogh, A.: (1919a) - The rate of diffusion of oxygen through animal tissue. *J. Phys.* 52, pp. 391-408,
- [22] Krogh, A. (1919b) - The supply of oxygen to tissue. *J. Phys.* 52 pp. 409-419.
- [23] Ling, S.C. & Atabek, H.B. (1973). Non linear analysis of pulsatile flow in arteries, *J. Fluid Mech* 155, pp. 275-511.
- [24] Li, C. W. and Chang, H.D. (1993) A non linear fluid model for pulmonary blood circulation. *J. Biomechanics*, Vol. 26, No. 6, pp. 653-664
- [25] Lutz, R.J. Hsu, L. Menawat, A., Zrubek, J. and Edwards, K. (1981) Fluid mechanics and boundary layer mass transport in an arterial model during steady and unsteady flow. Presented at 74th annual AIChE meeting., New Orleans.
- [26] Mac Donald, D.A.: (1960) Blood flow in arteries, Williams and Wilkins. Baltimore.
- [27] Mac Donald, D.A (1986) Pulsatile flow in catheterised artery. *J Biomechanics*, Vol, 19, No. 11, pp. 907-918.
- [28] Maithili Sharan; Jones, M.D. Jr.; Koehler R.c.; Traustman, R.J.; and Popel, A.S. (1989). A compartmental model for oxygen transport in brain micro-circulation, *annuals of Biomed Engg.* Vol. 17, pp. 907-918.